EUROPEAN ORGANIZATION FOR NUCLEAR RESEARCH

CERN-EP/82-54
10 May 1982

PHOTOPRODUCTION OF ρ^0 AND ω ON HYDROGEN AT PHOTON ENERGIES OF 20 TO 70 GeV

Bonn[1]-CERN[2]-Ecole Polytechnique[3]-Glasgow[4]-Lancaster[5]-Manchester[6]-Orsay[7]-Paris VI[8]-Paris VII[9]-Rutherford[10]-Sheffield[11] Collaboration

D. Aston[10], M. Atkinson[10], R. Bailey[11], A.H. Ball[6], H.J. Bautsch[1], B. Bouquet[7], G.R. Brookes[11], J. Bröring[1], P.J. Bussey[4], D. Clarke[10], A.B. Clegg[5], B. d'Almagne[7], G. de Rosny[3], B. Diekmann[1], A. Donnachie[6], M. Draper[4], B. Drevillon[3], I.P. Duerdoth[6], J.-P. Dufey[2], R.J. Ellison[6], D. Ezra[6], P. Feller[1], A. Ferrer[7], P.J. Flynn[5], W. Galbraith[11], R. George[8], S.D.M. Gill[6], M. Goldberg[8], S. Goodman[8], W. Graves[3], B. Grosstête[9], P.G. Hampson[6], K. Heinloth[1], R.E. Hughes-Jones[6], J.S. Hutton[10], M. Ibbotson[6], M. Jung[1], S. Katsanevas[3], M.A.R. Kemp[10], F. Kovacs[9], B.R. Kumar[10], G.D. Lafferty[6], J.B. Lane[6], J.-M. Lévy[8], V. Liebenau[1], J. Litt[10], G. London[9], D. Mercer[6], J.V. Morris[10], K. Müller[1], D. Newton[5], E. Paul[1], P. Petroff[7], Y. Pons[9], C. Raine[11], F. Richard[7], R. Richter[1], J.H.C. Roberts[6], P. Roudeau[7], A. Rougé[3], M. Rumpf[3], M. Sené[8], J. Six[7], I.O. Skillicorn[4], J.C. Sleeman[4], K.M. Smith[4], C. Steinhauer[1], K.M. Storr[5], R.J. Thompson[6], D. Treille[2], Ch. de la Vaissière[8], H. Videau[3], I. Videau[3], A.P. Waite[6], A. Wijangco[3], W. Wojcik[7], J.-P. Wuthrick[3] and T.P. Yiou[8]

(Submitted to Nuclear Physics B)

ABSTRACT

We present results on photoproduction of ρ^0 and ω in the reactions $\gamma p \to \pi^+\pi^- p$ and $\gamma p \to \pi^+\pi^-\pi^0 p$ by tagged photons in the energy range 20 to 70 GeV and 20 to 45 GeV, respectively. The production of the ρ^0 shows dominantly the characteristics of a diffractive process with respect to the E_γ and t dependence of the cross section and the spin density matrix. The ρ^0 photoproduction yields on average over the photon energy range a total cross section of $\sigma(\gamma p \to \rho^0 p) = (9.4 \pm 0.1)$ μb with an additional systematic error of ±1 μb, and average slope parameters of the t distribution $d\sigma/dt \sim \exp(-b|t| + ct^2)$, of $b = 9.1 \pm 0.1$ GeV^{-2} and $c = 3.1 \pm$ $\pm$ 0.2 GeV^{-4}. The shape of the ρ^0 peak in the $\pi^+\pi^-$ invariant mass spectra shows a skewing similar to that observed at lower energies. The photoproduction of ω is also consistent with a diffractive process and has a cross section of $\sigma(\gamma p \to \omega p) = (1.2 \pm 0.1)$ μb with an additional systematic error of ±0.2 μb. The average slope parameters of the t distribution are $b = 8.3 \pm 1.3$ GeV^{-2} and $c = 3.4 \pm 2.6$ GeV^{-4}.

1. INTRODUCTION

In this paper results are presented from a measurement of some 30,000 ρ^0 and 400 ω which were photoproduced in the reactions

$$\gamma p \to \rho^0 p \to \pi^+\pi^- p \qquad (1)$$

and

$$\gamma p \to \omega p \to \pi^+\pi^-\pi^0 p \qquad (2)$$

by photons in the energy range of 20 to 70 GeV. The data originate from a general study of photoproduction of multiparticle final states carried out at the CERN SPS using the OMEGA Spectrometer with a tagged photon beam (experiment WA4). From this experiment, a study of $\gamma p \to \pi^+\pi^- p$ concerned with the observation of the $\rho'(1600)$ decaying into $\pi^+\pi^-$ has been published[1].

Reactions (1) and (2) have been studied in detail at lower energies[2] and some results also exist from experiments with photons at higher energies[3-5]. These experiments show consistently that ρ^0 photoproduction at photon energies above the s-channel resonance region (> 2 GeV) has the characteristics of a diffractive process, i.e. a sharply forward peaked differential cross section varying slowly in magnitude with photon energy, and conservation of the s-channel helicity of the photon. In this experiment the ρ^0 photoproduction is studied in a photon energy range between the bulk of data (for E < 20 GeV) and the first high energy measurements ($50 < E_\gamma < 200$ GeV). In the case of ω photoproduction it was found from the energy dependence of the cross section that unnatural parity exchange (pion exchange) is an important contribution at lower photon energies[6]. For the photon energies considered in the present experiment nondiffractive contributions should be small, so that more similarities between ρ^0 and ω photoproduction are expected.

2. EXPERIMENTAL SET-UP AND DATA

The apparatus used was the OMEGA Spectrometer at the CERN SPS, with a tagged photon beam spanning the energy range 20 to 70 GeV. A full account of the beam and the particle detection can be found elsewhere[7]. The trigger on events of the reactions considered here required two charged

particles to traverse the spectrometer in the forward direction and at least one hit in a scintillation counter surrounding the hydrogen target. Electromagnetic background was reduced, by a system of veto counters in the electromagnetic plane, to a level below 1% of the e^+e^- pair cross section. Charged particles were identified by means of a Cerenkov counter with thresholds of 5.9, 19 and 36 GeV/c for pions, kaons and $\bar{p}/p$, respectively. Photons (from π^0 meson decays) were measured by a downstream photon detector consisting of an active converter of lead-glass slabs, a position detector made of scintillation fingers and a large totally absorbing lead glass array. This calorimeter subtended a solid angle of 0.4 steradian about the forward direction and measured photons above 500 MeV, giving the photon direction to an accuracy of 0.2 mrad.

From the interactions of 2.2×10^{10} photons within the tagging energy range, incident on 2.76×10^{24} protons/cm^2 of the hydrogen target, a total of 5×10^5 events were recorded with this trigger. In the data reduction we required one or two positively charged particles, one negatively charged particle and zero or one π^0 to be fitted to a vertex within the hydrogen target. For events with one positively charged particle we assumed that the missing particle was the recoil proton, while for events with two positively charged particles we defined the lowest momentum particle to be the recoil proton and only accepted the event if this particle had a momentum below 1.5 GeV/c and a laboratory angle with respect to the photon direction greater than 55°. The remaining background of misidentified pions was estimated to be less than 10%. The two charged tracks that passed through the Cerenkov counter (acceptance window required momentum $p \geq 3$ GeV/c) had to be consistent with being a $\pi^+\pi^-$ pair. In addition we required a well-measured primary photon with energy greater than 20 GeV.

To eliminate electromagnetic background in reaction (1) the pions were required to make an angle greater than 4 mrad with the electromagnetic plane.

Figures 1 and 2 show the distribution of ΔE = incident beam energy - sum of pion energies - proton kinetic energy*), separately for the candidates

*) When the proton is observed.

of reactions (1) and (2). In order to remove background from other reactions we accepted only the events with $\Delta E < 3$ GeV for reaction (1) and $\Delta E < 5$ GeV for reaction (2). In the final samples we obtained 33,000 events of the reaction $\gamma p \to p\pi^+\pi^-$ and 1099 events of the reaction $\gamma p \to$ $\to p\pi^+\pi^-\pi^0$.

3. EXPERIMENTAL RESULTS

3.1 ρ^0 photoproduction in the reaction $\gamma p \to p\pi^+\pi^-$

In Fig. 3 we show the $\pi^+\pi^-$ mass spectrum of reaction (1) for three intervals of photon energy and for the total energy range. The data are corrected for the mass dependent geometrical acceptance of the apparatus (dashed lines in Fig. 3). The acceptance was calculated by a Monte-Carlo simulation of events of reaction (1) for various mass values of the $\pi^+\pi^-$ system. The main inputs to the simulation were a photon bremsstrahlung spectrum as measured, a production cross section independent of the photon energy with a dependence on the four-momentum transfer squared $d\sigma/dt \sim$ $\sim \exp(-9|t|)$, and a polar decay angular distribution of the $\pi^+\pi^-$ system in the s-channel helicity frame, $W(\cos\theta) \sim \sin^2\theta$. These assumptions are supported by previous experiments[6].

The ρ^0 signal was analysed by fitting the mass spectra in the range $0.56 < m(\pi^+\pi^-) < 0.92$ GeV with the following two expressions:

$$d\sigma/dm = f_\rho \sigma_\rho(m)(m_\rho/m)^n + f_{BG} PS(m)$$

with

$$\sigma_\rho(m) = \frac{m}{\pi} \frac{\Gamma_\rho(m)}{(m_\rho^2 - m^2)^2 + m_\rho^2 \Gamma_\rho^2(m)} \quad ; \quad \Gamma_\rho(m) = \Gamma_0 (q/q_\rho)^3 \qquad (3)$$

and PS(m) is a second order polynomial in m, q is the pion momentum in the centre of mass of the dipion system and Γ_0 is the ρ width; ρ subscripts for m and q refer to the nominal value of the dipion mass; and

$$d\sigma/dm = f_\rho \sigma_\rho(m) + f_I I(m) + f_{BG} PS(m)$$

with

$$I(m) = \frac{m^2 - m_\rho^2}{(m_\rho^2 - m^2)^2 + m_\rho^2 \Gamma_\rho^2(m)} \, . \qquad (4)$$

Optionally we have taken into account $\rho^0\omega$ interference by replacing $\sigma_\rho(m)$ by $\sigma_{\rho\omega}(m) = \left[BW_\rho(m) + \alpha \exp(i\beta)\, BW_\omega(m)\right]^2$ where $BW_\rho^2(m) = \sigma_\rho(m)$ and $BW_\omega(m)$ is the relativistic Breit-Wigner amplitude of the ω meson and α and β are real parameters to be determined in the fit.

Equation (3) represents the fitting of the $\pi^+\pi^-$ cross section by a ρ^0-production term, where the resonance formula is modified by a phenomenological Ross-Stodolsky factor[8] $(m_\rho/m)^n$, plus a general background. This factor was used previously to account for the skewing of the shape of the ρ^0 signal[2]. Equation (4) represents another commonly accepted fit procedure with the ρ^0 shape distortion accounted for by an interference term[9,10].

Results of the fits are collected in Table 1. The curves in Figs. 3a, b and c correspond to the fits according to Eq. (3), whereas in Fig. 3d we show the fit result according to Eq. (4). It is found that the fit fails to describe the ρ^0 peak region $\left[0.72 < m(\pi^+\pi^-) < 0.78 \text{ GeV}\right]$. The inclusion of a $\rho\omega$ interference term in the fit gives the expected values for the parameters α and β [11]; however, it does not improve the goodness of the fit significantly. From the fits due to both hypotheses [Eqs. (3) and (4)] we conclude that the magnitude of the skewing effect is similar to that at lower energies, i.e. it does not depend on the photon energy in the range covered here. Values of the "Ross-Stodolsky" exponent n as a function of t obtained in further fits [Eq. (3)] are shown in Fig. 4.

Estimates of the total ρ^0 cross section obtained from fits to the $\pi^+\pi^-$ mass spectrum are given in Table 2 together with estimates calculated from the peak cross section by applying the method of Spital and Yennie[12], and from the experimental spherical harmonic moment $\langle Y_2^0 \rangle$ as function of the $\pi^+\pi^-$ mass by assuming that ρ^0 is only produced with conservation of s-channel helicity (see below). The values in Table 2 are fully corrected with respect to acceptance losses, in particular also for the loss in the low t region (which is significant for $|t| < 0.06$ GeV^2, see Fig. 5).

In Section 4 we use the total ρ^0 production cross section obtained from the fit according to Eq. (4).

In Fig. 5 we show $d\sigma/dt$ averaged over the ρ^0 mass region $[0.56 < m(\pi^+\pi^-) < 0.92$ GeV$]$ for three intervals of photon energy. The distributions were fitted to $d\sigma/dt = a \exp(-b|t| + ct^2)$ in the t range $0.06 < |t| < 1.0$ GeV^2. The values of b and c found in the fits are shown in Table 3. On average over the whole range of photon energy (20-70 GeV) we found: $b = 9.1 \pm 0.1$ GeV^{-2} and $c = 3.1 \pm 0.2$ GeV^{-4}. These slope parameters are consistent with previous photoproduction experiments (see Section 4) and also with hadron induced elastic processes[13].

Figure 6 shows the slope parameter b as function of $M(\pi^+\pi^-)$ determined in the range $0.06 < |t| < 0.3$ GeV^2 with c fixed at zero (see Table 3). The mass dependence observed is similar to that for the corresponding t range in hadron induced diffractive production at high energies[14].

We now consider the decay angular distribution of the ρ^0 in the s-channel helicity frame. We use angles θ and ϕ as defined in Fig. 211 of Ref. 2. The two-dimensional $\cos\theta,\phi$ distribution was corrected for acceptance losses in steps of $\cos\theta$ and ϕ. (It was found that a step size of 0.2 for $\cos\theta$ and $\pi/5$ for ϕ was sufficient.)

Spherical harmonic moments $\langle Y_\ell^m \rangle$ were studied as a function of $M(\pi^+\pi^-)$ for ℓ up to 4. In Fig. 7 we show (normalized to $\langle Y_0^0 \rangle$) $\langle Y_2^0 \rangle$ and in addition $\langle Y_2^1 \rangle$ and $\langle Y_2^2 \rangle$ which are sensitive to helicity flip contributions. All other moments were found to be consistent with zero. A dominant $\langle Y_2^0 \rangle$ is observed; the moment is expected to be the only non-vanishing contribution (besides $\langle Y_0^0 \rangle$) in the case of strict s-channel helicity conservation (SCHC).

The moments were also determined as function of t averaging over the events in a reduced ρ^0 mass range $[0.6 < M(\pi^+\pi^-) < 0.9$ GeV$]$. Figure 8 shows the ρ_{00}, ρ_{1-1} and Re ρ_{10} computed from these moments according to

$$\rho_{00} = \frac{1}{3}\left(\sqrt{5}\,\frac{\langle Y_2^0\rangle}{\langle Y_0^0\rangle} + 1\right)$$

$$\rho_{1-1} = -\sqrt{\frac{5}{12}}\,\mathrm{Re}\,\frac{\langle Y_2^2\rangle}{\langle Y_0^0\rangle}$$

$$\mathrm{Re}\,\rho_{10} = \sqrt{\frac{5}{24}}\,\mathrm{Re}\,\frac{\langle Y_2^1\rangle}{\langle Y_0^0\rangle}\,.$$

All three spin density matrix elements must vanish if s-channel helicity conservation is strictly valid. The data agree in general with this assumption. The observed deviation from SCHC could be due to contamination by remaining e^+e^- pairs in the data set, so we cannot draw any conclusion about minor contributions from spin flip processes.

3.2 ω production in the reaction $\gamma p \to \pi^+\pi^-\pi^0 p$

The reaction $\gamma p \to \pi^+\pi^-\pi^0 p$ was analysed in the photon energy range $20 < E_\gamma < 45$ GeV. The $\pi^+\pi^-\pi^0$ mass spectrum of reaction (2) is shown in Fig. 9 together with the acceptance assuming SCHC (the low acceptance and the limitation to $E_\gamma < 45$ GeV stems from the restricted π^0 detection). There is a strong signal at the ω mass and an indication of ϕ production of approximately the correct magnitude known from the ϕ decay into $\pi^+\pi^-\pi^0$ [see for instance Ref. (3)]. The non-ω contribution in the ω mass range was estimated to be 10% by fitting the ω signal together with a linearly rising background in the mass region $0.72 < m(\pi^+\pi^-\pi^0) < 0.84$ GeV. The ω production cross section was calculated from the estimated number of ω in the $\pi^+\pi^-\pi^0$ mass spectrum. In average over the energy range considered we find: $\sigma \times BR(\omega \to \pi^+\pi^-\pi^0) = 1.03 \pm 0.1$ μb with an additional systematic uncertainty of 0.2 μb.

For further studies of the ω we selected all the events in the above mass region neglecting background contributions. The t-dependence of the ω is shown in Fig. 10. The result of a fit to $d\sigma/dt = a \exp(-b|t| + ct^2)$ is given in Table 3.

The decay angular distributions of the ω signal in the s-channel helicity system are shown in Fig. 11. The cos θ distribution*), is consistent with a purely $\sin^2\theta$ dependence (a fit gave a χ^2/d.o.f. of 0.82) and the azimuthal distribution is flat. Such distributions are expected in the case of an SCHC production mechanism. The spin density matrix elements of spin 1 were calculated from Fig. 11 yielding

---

*) θ is the polar angle measured between the normal to the decay plane in the $\pi^+\pi^-\pi^0$ centre of mass system and the direction of the recoil proton in the overall centre of mass system.

$$\rho_{00} = 0.1 \pm 0.2 \quad \rho_{1-1} = 0.0 \pm 0.5 \quad \text{Re}\ \rho_{10} = 0.0 \pm 0.1$$

i.e. they are consistent with zero.

4. COMPARISONS WITH ADDITIVE QUARK MODEL PREDICTIONS

From the additive quark model we expect the vector meson production cross sections to be related to the πp elastic scattering amplitudes. Assuming the validity of diagonal vector meson dominance one may write

$$\sigma(\gamma p \to \rho^0 p) = \frac{\alpha\pi}{\gamma_\rho^2}\,\sigma^{el}(\rho^0 p) = \frac{\alpha\pi}{2\gamma_\rho^2}\left[\sigma^{el}(\pi^+ p) + \sigma^{el}(\pi^- p)\right]$$

$$\sigma(\gamma p \to \omega p) = \frac{\alpha\pi}{\gamma_\omega^2}\,\sigma^{el}(\omega p) = \frac{\alpha\pi}{2\gamma_\omega^2}\left[\sigma^{el}(\pi^+ p) + \sigma^{el}(\pi^- p)\right] .$$

It has already been shown with high-energy data[3] that such predictions describe the energy dependence of the total elastic cross sections well; this implies that the photoproduction data at high energies are consistent with an energy independent photon-vector meson coupling constant. Our values of total cross sections are in agreement with this result.

On the basis of the quark model relations the forward cross sections for ω and ρ^0 are used to calculate $\gamma_\omega^2/4\pi$, the photon ω coupling strength, assuming that $\gamma_\rho^2/4\pi$ is known. Setting $\gamma_\rho^2/4\pi = 0.64 \pm 0.1$ from e^+e^- annihilations[2] we find $\gamma_\omega^2/4\pi = 6.4 \pm 1.8$. This value is in agreement with the value of (4.6 ± 0.5) from e^+e^- annihilation and with other estimates from photoproduction on complex nuclei [7.5 ± 1.3, if the ratio of real to imaginary part of the scattering amplitude is $\eta_\omega = -0.2$ [2]] and from quark model predictions assuming diagonal vector meson dominance [5.4 ± 0.4 [4]].

Figure 12 shows compilations of the slope parameter b and the forward cross section $d\sigma/dt$ at $t = 0$ from photoproduction of ρ^0 and ω in comparison with quark model predictions according to the above relations. The πp elastic data were taken from recent high-energy measurements[13] and, for the lower energies, from a compilation by Leith[15]. The forward cross sections of ρ^0 and ω in this experiment were calculated from total cross sections and slope parameters b, where we used the b values from the fits to the restricted t-range, with c fixed to zero (see Table 3). For calculating

the forward cross section from πp data we imposed $\gamma_\rho^2/4\pi = 0.64$ and $\gamma_\omega^2/4\pi = 6.4$. Within the limits of the experimental errors good agreement is observed between ρ^0 and ω on one hand, and between both of these and the πp calculation on the other. This result supports the earlier conclusion based on the comparison of total cross sections only[16].

5. SUMMARY

From our study of photoproduction of ρ^0 and ω on hydrogen in the photon energy range of 20 to 70 GeV we note the following facts:

i) The production of ρ^0 and ω shows dominantly the characteristics of a diffractive process.

ii) $\sigma(\gamma p \to \rho^0 p) = 9.4 \pm 0.1 \pm 1$ μb on average over $20 < E_\gamma < 70$ GeV and $\sigma(\gamma p \to \omega p) BR(\pi^+\pi^-\pi^0) = 1.03 \pm 0.1 \pm 0.2$ μb on average over $20 < E_\gamma < 45$ GeV *).

iii) The t distributions fitted to $d\sigma/dt \sim \exp(-b|t| + ct^2)$ yield the average slope parameters $b = 9.1 \pm 0.1$ GeV^{-2} and $c = 3.1 \pm 0.2$ GeV^{-4} for the ρ^0 and $b = 8.3 \pm 1.3$ GeV^{-2} and $c = 3.4 \pm 2.6$ GeV^{-4} for the ω.

iv) The shape of the ρ^0 peak in the $\pi^+\pi^-$ invariant mass spectrum shows a skewing previously observed at lower energies. By quantitative comparisons it was found that there is no significant difference with the shape observed at lower energies. This means that the main ideas for explaining it, for instance the Söding interference model, appear to be valid.

v) The forward cross section and the slope parameter b of ρ and ω agree with predictions derived using simple vector meson dominance from measurements of pion elastic scattering by assuming naive quark model relations.

---

*) In both the results the first error is that due to statistics and the second is the systematic error due to normalization uncertainties.

Acknowledgements

We are grateful to CERN for providing the facilities, and especially to the Omega Group for their help in operating the spectrometer, and the DD Division for providing on-line and off-line software. We have also benefitted from the work of technical staff in our home institutions. We acknowledge financial support from the Science Research Council, from the Institut National de Physique Nucléaire et de Physique des Particules, and from the Bundesministerium für Wissenschaft und Forschung.

REFERENCES

1) D. Aston et al., Phys. Lett. 93B (1980) 215.

2) For a review of these experiments, see
T.H. Bauer, R.D. Spital, D.R. Yennie and F.M. Pipkin, Rev. Mod. Phys. 50 (1978) 261.

3) R.M. Egloff et al., Phys. Rev. Lett. 43 (1979) 657.

4) R.M. Egloff et al., Phys. Rev. Lett. 43 (1979) 1545.

5) A.M. Breakstone et al., Proc. 20th Int. Conf. on High-Energy Physics, Madison 1980, p. 233.

6) J. Ballam et al., Phys. Rev. D 7 (1973) 3150, and D 8 (1973) 1277.

7) D. Aston et al., Nucl. Phys. B116 (1980) 1.
D. Aston et al., Nucl. Instrum. Methods (to be published).

8) R. Ross and V. Stodolsky, Phys. Rev. 149 (1966) 1172.

9) P. Söding, Phys. Lett. 19 (1966) 702.

10) H. Alvensleben et al., Phys. Rev. Lett. 18 (1969) 1058 and Phys. Rev. Lett. 26 (1971) 273.

11) Review of Particle Properties, Rev. Mod. Phys. 52 (1980) 2.

12) R. Spital and D.R. Yennie, Phys. Rev. D 9 (1974) 126.

13) D.B. Ayres et al., Phys. Rev. D 15 (1977) 3105.

14) U. Amaldi et al., Rev. Nucl. Sci. 26 (1976) 365.

15) D.W.G.S. Leith, Electromagnetic interactions of hadrons, Vol. 1, Plenum Press, NY, 1979, p. 345 (Eds. A. Donnachie and G. Shaw).

16) A.M. Eisner, Proc. Int. Symp. on Lepton and Photon Interactions at High Energies, 1979 (FNAL-Pub., Batavia, 1979), p. 448.

17) R. Giese, Stanford University Thesis, 1974 (unpublished).

18) C. Berger et al., Phys. Lett. B39 (1972) 659.

19) G. McClellon et al., Phys. Rev. Lett. 22 (1969) 374.

20) H. Alvensleben et al., Nucl. Phys. B18 (1970) 333.

21) Y. Eisenberg et al., Phys. Rev. D 5 (1972) 15.

22) G. Gladding et al., Phys. Rev. D 8 (1973) 3721.

23) D. Benaksas et al., Phys. Lett. 39B (1972) 289.

Table 1

Results from fits of the ρ^0 peak
in the range $0.56 < M(\pi^+\pi^-) < 0.92$ GeV

	Eq. (3) (Ross-Stodolsky)	Eq. (4) (Söding)	Eq. (4) + ω interference
E_γ: 20-70 GeV			
m_ρ (GeV)	0.758 ± 0.003	0.753 ± 0.009	0.747 ± 0.004
Γ_0 (GeV)	0.141 ± 0.018	0.137 ± 0.019	0.135 ± 0.02
$\alpha = \lvert BW_\omega \rvert / \lvert BW_\rho \rvert$	-	-	0.013 ± 0.002
$\rho\omega$ rel. phase β (°)	-	-	89.9 ± 1.0
n	4.4 ± 0.1	-	-
E_γ: 20-30 GeV			
m_ρ (GeV)	0.771 ± 0.011	0.761 ± 0.001	
Γ_0 (GeV)	0.141 ± 0.020	0.128 ± 0.01	
n	4.7 ± 0.1	-	
E_γ: 30-45 GeV			
m_ρ (GeV)	0.771 ± 0.010	0.766 ± 0.001	
Γ_0 (GeV)	0.141 ± 0.038	0.138 ± 0.01	
n	4.4 ± 0.1	-	
E_γ: 45-70 GeV			
m_ρ (GeV)	0.773 ± 0.005	0.765 ± 0.001	
Γ_0 (GeV)	0.149 ± 0.034	0.116 ± 0.02	
n	4.1 ± 0.1	-	

Table 2

Total cross section for the reaction $\gamma p \to \rho^0 p$ in μb. The systematic error due to normalization uncertainties is estimated to be ±1 μb (not included here).

Hypothesis \ E_γ (GeV)	20-70	20-30	30-45	45-70
Eq. (3)	9.2 ± 0.1	8.8 ± 0.1	9.6 ± 0.1	7.5 ± 0.1
Eq. (4)	9.4 ± 0.1	8.5 ± 0.1	9.7 ± 0.1	5.8 ± 0.1
$\frac{1}{2}\pi\Gamma_\rho \left.\frac{d\sigma}{dm}\right\|_{m=m_\rho}$ *)	9.6 ± 0.1	9.7 ± 0.1	9.5 ± 0.1	7.7 ± 0.1
$-\sqrt{20\pi} \times \langle Y_2^0 \rangle$	8.1 ± 0.05	11.0 ± 0.1	8.9 ± 0.1	5.0 ± 0.05

*) We used m_ρ = 0.772 GeV and Γ_ρ = 0.136 GeV as obtained in an e^+e^- colliding beam experiment[23].

Table 3

Slope parameters from a fit to the ρ^0 and ω data of the form $d\sigma/dt = a \exp(-b|t| + ct^2)$ and the forward differential cross sections $d\sigma/dt_{t=0}$.

		b (GeV^{-2})	c (GeV^{-4})	$\left.\frac{d\sigma}{dt}\right\|_{t=0}$ (nb GeV^{-2})	t range (GeV^2)
ρ^0	20 < E_γ < 30 GeV	9.7 ± 0.2	3.8 ± 0.2	82.5 ± 12	0.06-1
		7.6 ± 0.2	0 (fixed)	84.4 ± 27	0.06-0.3
	30 < E_γ < 45 GeV	9.0 ± 0.2	2.7 ± 0.2	87.3 ± 15	0.06-1
		7.8 ± 0.1	0 (fixed)	82.7 ± 25	0.06-0.3
	45 < E_γ < 70 GeV	10.0 ± 0.2	4.3 ± 0.2	58 ± 17	0.06-1
		8.4 ± 0.1	0 (fixed)	62.2 ± 19	0.06-0.3
ω	20 < E_γ < 45 GeV	8.3 ± 1.3	3.4 ± 2.6	9.4 ± 1.3	0.06-0.8

Figure captions

Fig. 1 : Distribution of ΔE (see text) for reaction $\gamma p \to \pi^+\pi^- p$.

Fig. 2 : Distribution of ΔE for reaction $\gamma p \to \pi^+\pi^-\pi^0 p$. The $\pi^+\pi^-\pi^0$ mass was restricted to the range $0.72 < m < 0.84$ GeV.

Fig. 3 : a)-c): $M(\pi^+\pi^-)$ from $\gamma p \to \pi^+\pi^- p$. The full lines correspond to the fit according to Eq. (3) (see Table 1). a) $20 < E_\gamma < 30$ GeV; b) $30 < E_\gamma < 45$ GeV; c) $45 < E_\gamma < 70$ GeV. The dashed lines indicate the geometrical acceptance. d) $M(\pi^+\pi^-)$ from $\gamma p \to \pi^+\pi^- p$ for all photon energies ($20 < E_\gamma < 70$ GeV). The full line corresponds to a fit according to Eq. (4); the dashed line and the dotted line correspond to the contributions from I(m) and PS(m), respectively.

Fig. 4 : The parameter n as function of t from fits according to Eq. (3), $\gamma p \to \pi^+\pi^- p$.

Fig. 5 : $d\sigma/dt$ averaged over the range $0.55 < M(\pi^+\pi^-) < 0.95$ GeV for three intervals of photon energy. a) $20 < E_\gamma < 30$ GeV; b) $30 < E_\gamma < 45$ GeV; c) $45 < E_\gamma < 70$ GeV. The errors are explained in the text.

Fig. 6 : The slope parameter b as a function of $M(\pi^+\pi^-)$ for $\gamma p \to \pi^+\pi^- p$.

Fig. 7 : Normalized spherical harmonic moments as a function of $M(\pi^+\pi^-)$ from $\gamma p \to \pi^+\pi^- p$. The angles are defined in the s-channel helicity frame.

Fig. 8 : Spin density matrix elements as a function of t averaged over the ρ^0 mass range $[0.6 < M(\pi^+\pi^-) < 0.9$ GeV$]$, $\gamma p \to \pi^+\pi^- p$.

Fig. 9 : $M(\pi^+\pi^-\pi^0)$ from reaction $\gamma p \to \pi^+\pi^-\pi^0 p$: $20 < E_\gamma < 45$ GeV; the dashed curve indicates the geometrical acceptance.

Fig. 10 : $d\sigma/dt$ for $\gamma p \to \omega p$ $[0.72 < M(\pi^+\pi^-\pi^0) < 0.84$ GeV$]$.

Fig. 11 : Decay angular distributions of the ω signal in the s-channel helicity frame. a) $\cos\theta$ distribution; b) ϕ distribution. The curve in (a) corresponds to a $\sin^2\theta$ dependence.

Fig. 12 : a) Forward cross section and b) slope parameters b of ρ^0 and ω in comparison to other experiments and the quark model predictions deduced from πp elastic data (see text). The ω cross sections were multiplied by an appropriate factor (of ~ 8) accounting for the total cross section ratio of ρ^0 and ω photoproduction. The curve in (a) was determined by means of the expression $\alpha\pi/2\gamma_\rho^2[d\sigma(\pi^+p \to \pi^+p)/dt + d\sigma(\pi^-p \to \to \pi^-p)/dt]$ at $t = 0$. The curve in (b) was derived from $\frac{1}{2}[b(\pi^+p \to \pi^+p) + b(\pi^-p \to \pi^-p)]$. The symbols correspond to the following references for $\gamma p \to \rho^0 p$: x [18,19], + [21], ▼ [6], ▲ [22], ■ [17], ♦ [20], ● this experiment, and for $\gamma p \to \omega p$: □ [4], Δ [5], ○ this experiment.

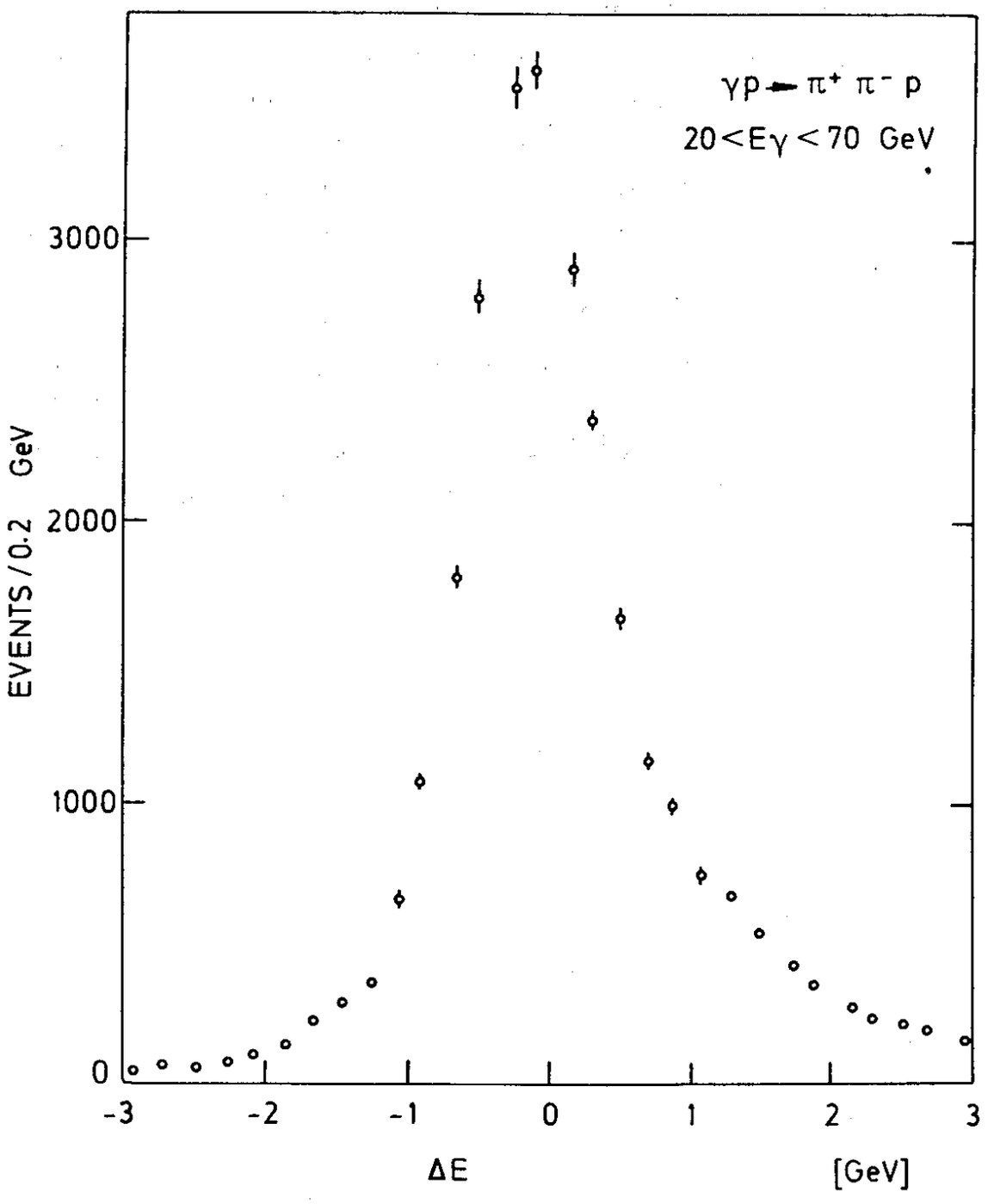
γp → π⁺ π⁻ p
20<Eγ<70 GeV
EVENTS / 0.2 GeV
3000
2000
1000
0
-3
-2
-1
0
1
2
3
ΔE
[GeV]

Fig. 1

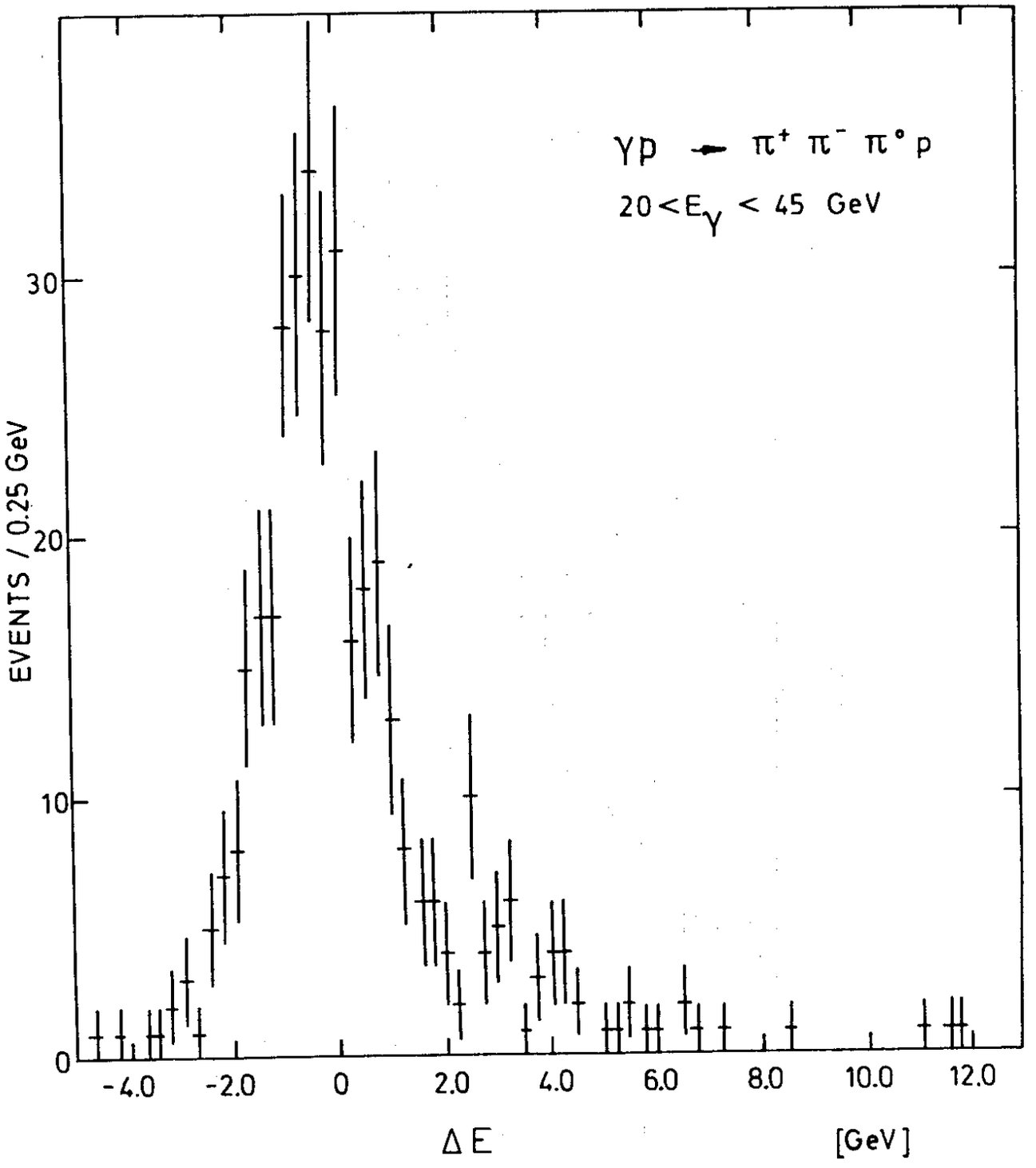
γp → π⁺ π⁻ π° p
20 < Eγ < 45 GeV
EVENTS / 0.25 GeV
30
20
10
0
-4.0
-2.0
0
2.0
4.0
6.0
8.0
10.0
12.0
ΔE
[GeV]

Fig. 2

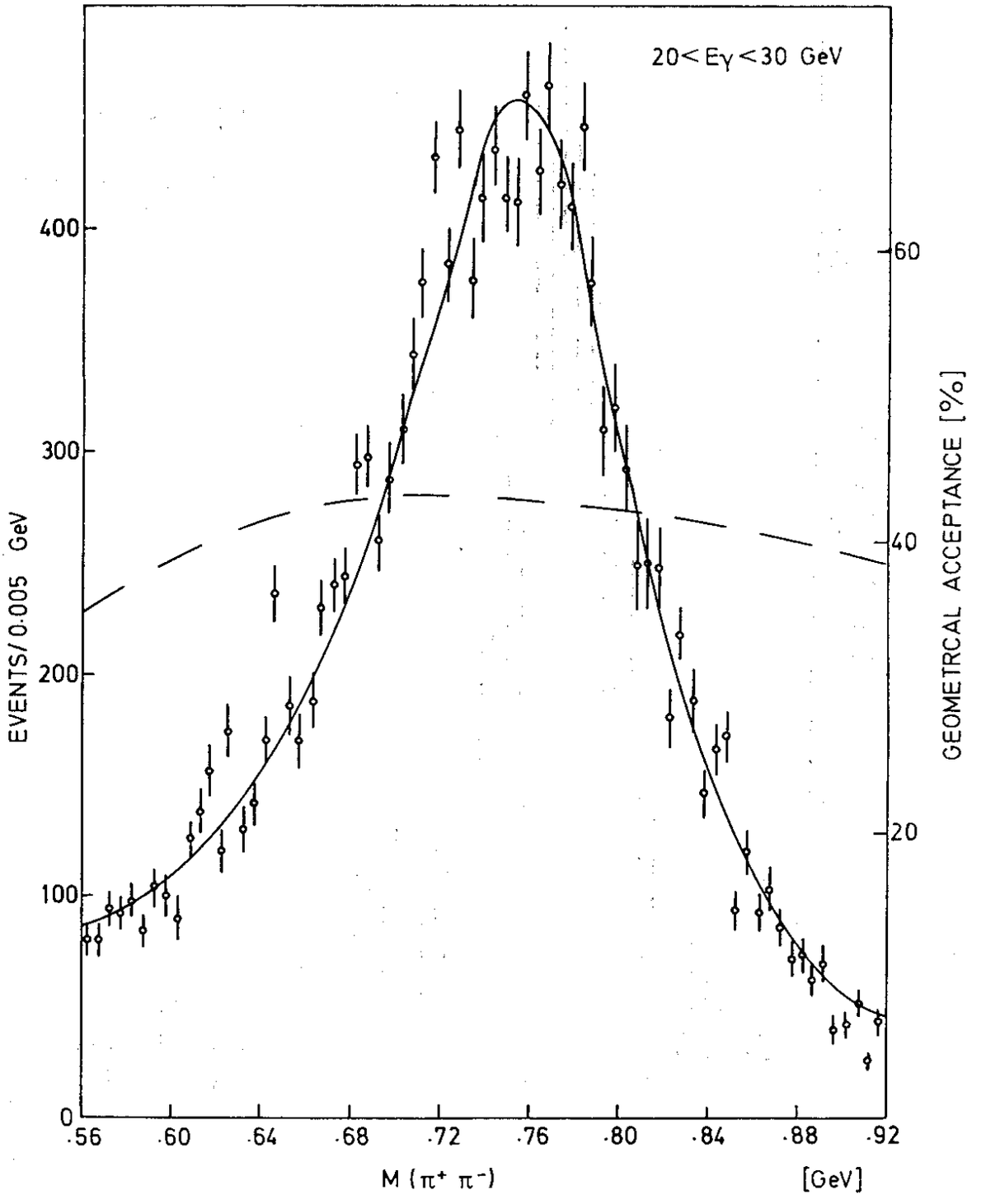
20< Eγ <30 GeV
EVENTS/0.005 GeV
GEOMETRCAL ACCEPTANCE [%]
M (π+ π-)
[GeV]
0
100
200
300
400
20
40
60
.56
.60
.64
.68
.72
.76
.80
.84
.88
.92

Fig. 3a

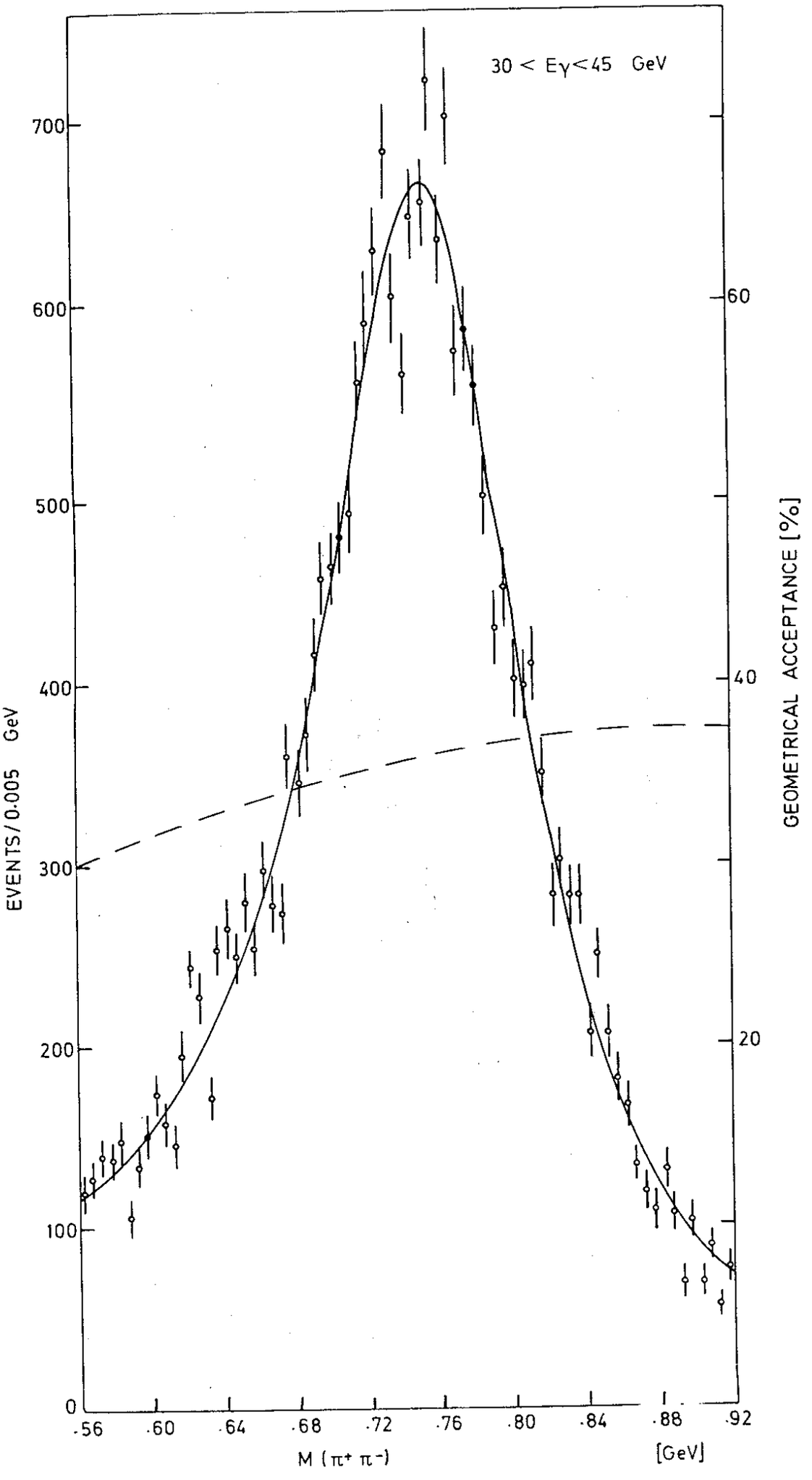
30 < Eγ<45 GeV
EVENTS/0.005 GeV
GEOMETRICAL ACCEPTANCE [%]
M (π⁺ π⁻)
[GeV]
0
100
200
300
400
500
600
700
20
40
60
.56
.60
.64
.68
.72
.76
.80
.84
.88
.92

Fig. 3b

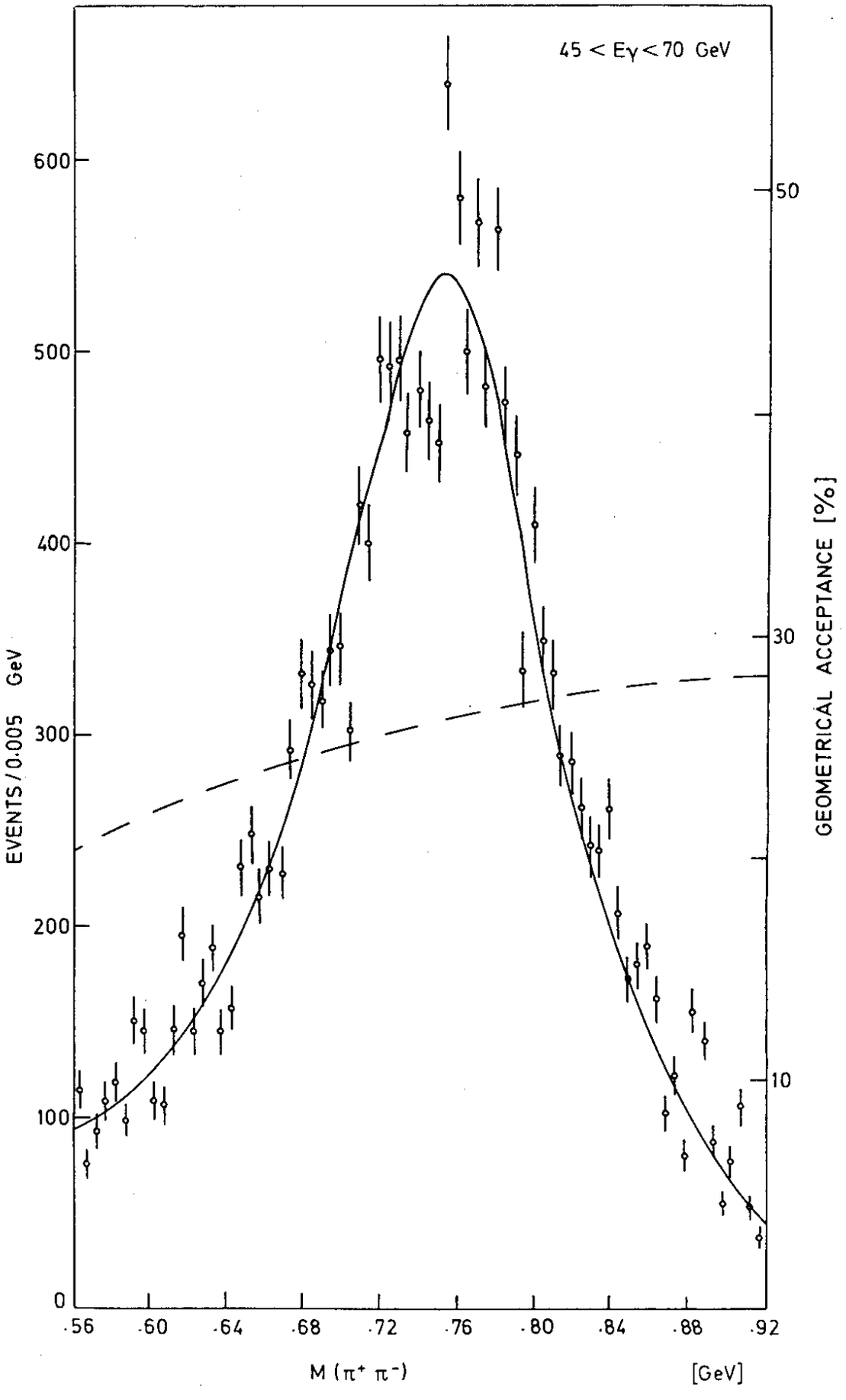
45 < Eγ < 70 GeV
EVENTS / 0.005 GeV
GEOMETRICAL ACCEPTANCE [%]
M (π⁺ π⁻)
[GeV]
0
100
200
300
400
500
600
10
30
50
.56
.60
.64
.68
.72
.76
.80
.84
.88
.92

Fig. 3c

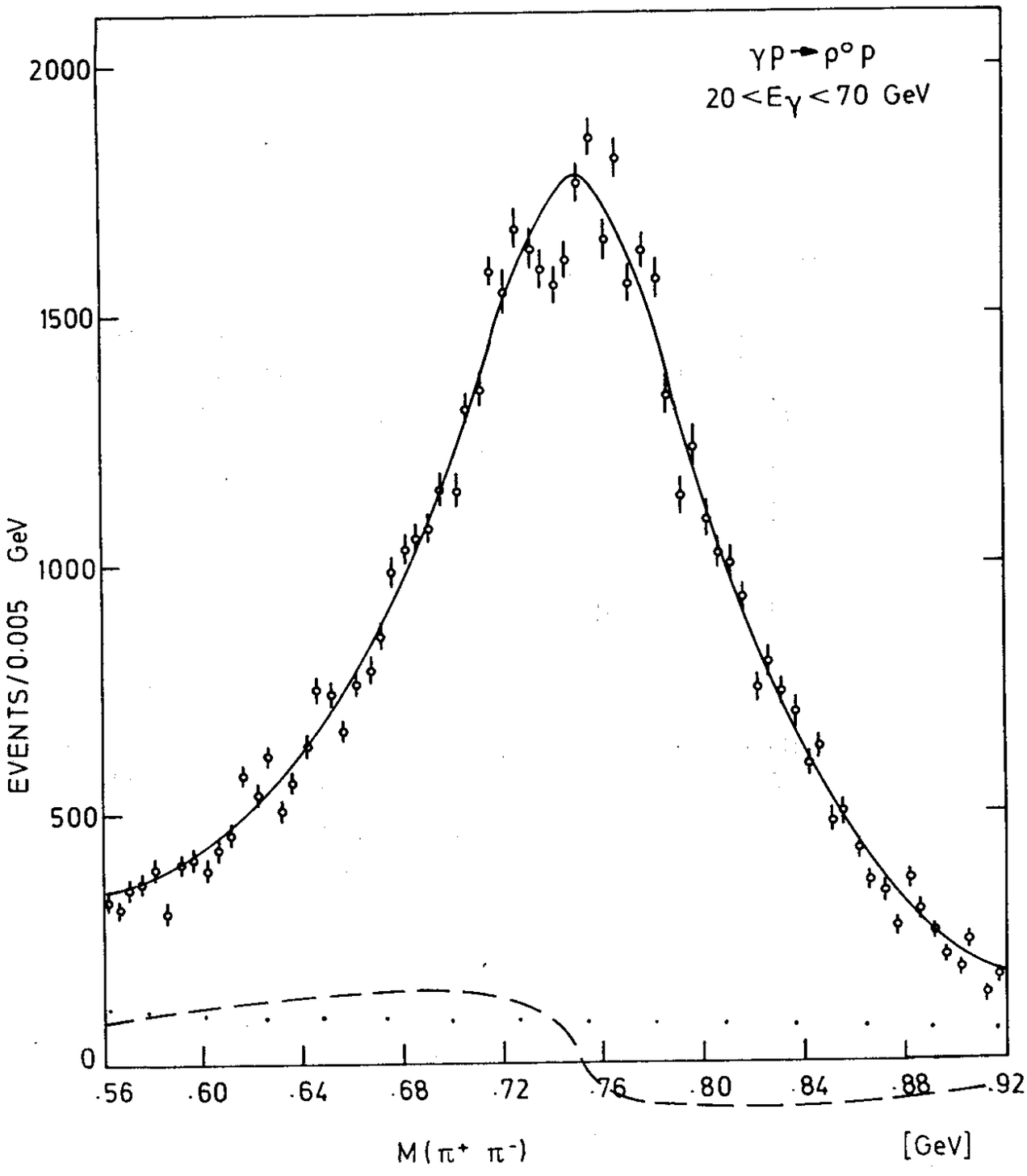
γp → ρ° p
20 < Eγ < 70 GeV
2000
1500
1000
500
0
EVENTS/0.005 GeV
.56
.60
.64
.68
.72
.76
.80
.84
.88
.92
M(π⁺ π⁻)
[GeV]

Fig. 3d

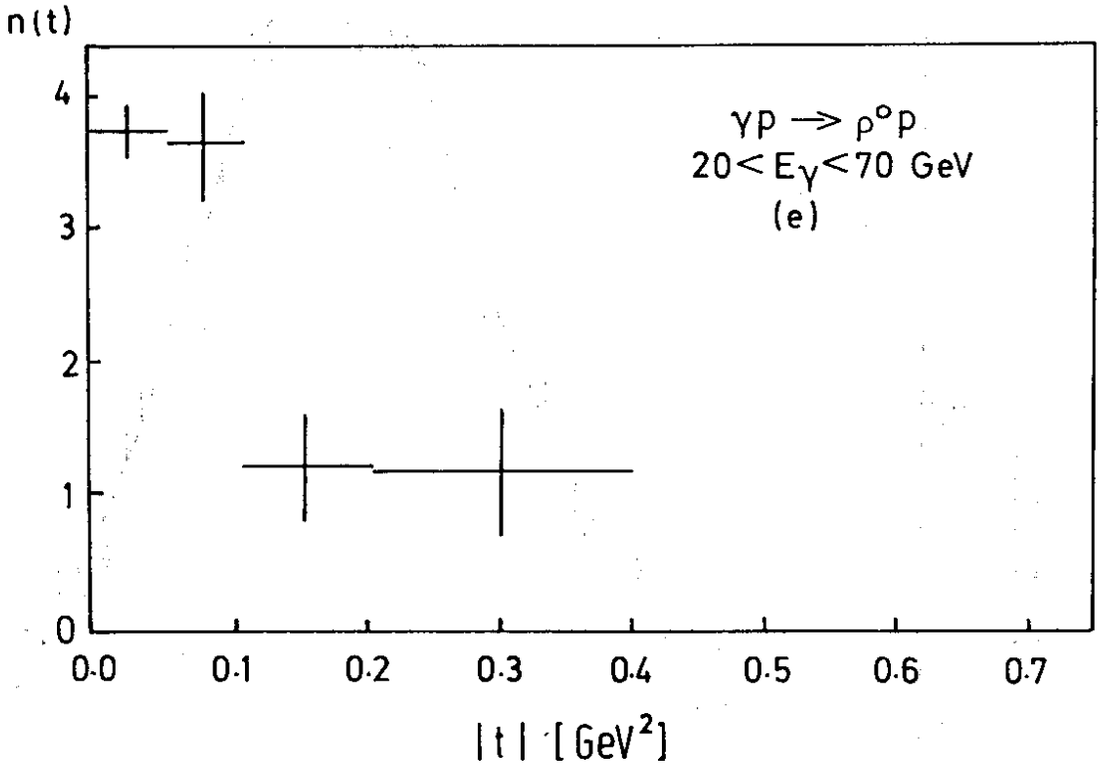

Fig. 4

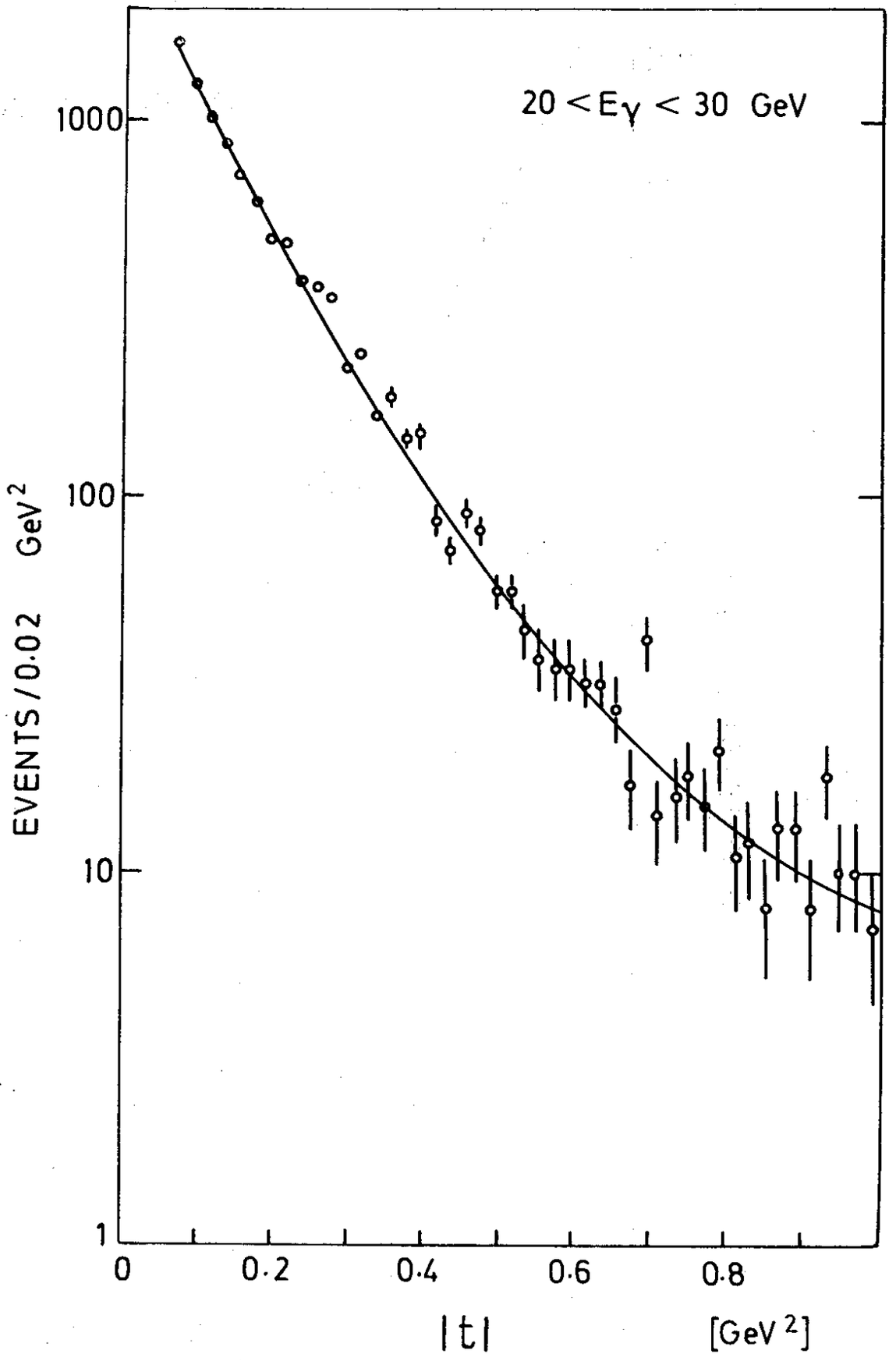

Fig. 5a

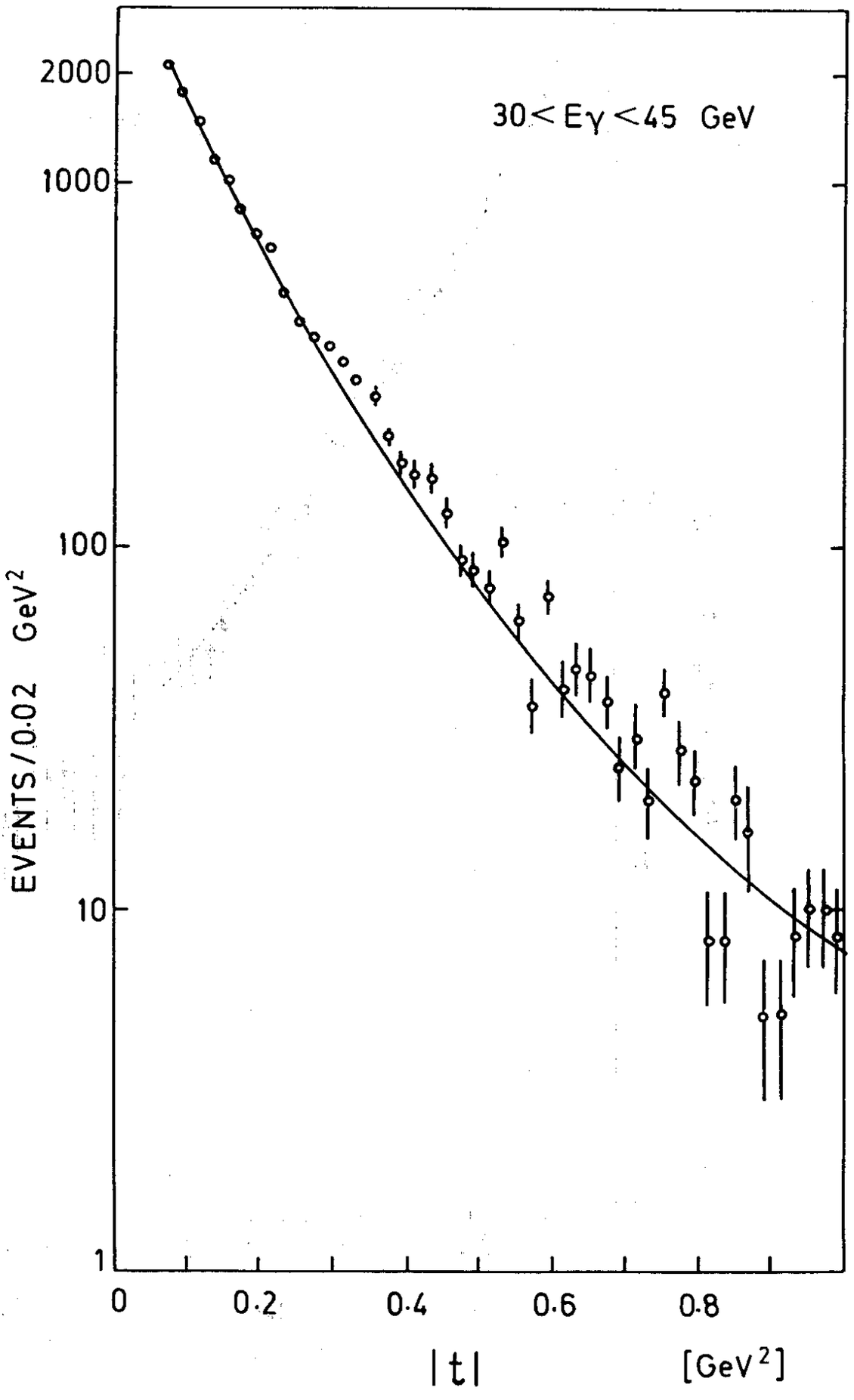
30 < Eγ < 45 GeV
2000
1000
100
10
1
EVENTS/0.02 GeV²
0
0.2
0.4
0.6
0.8
|t|
[GeV²]

Fig. 5b

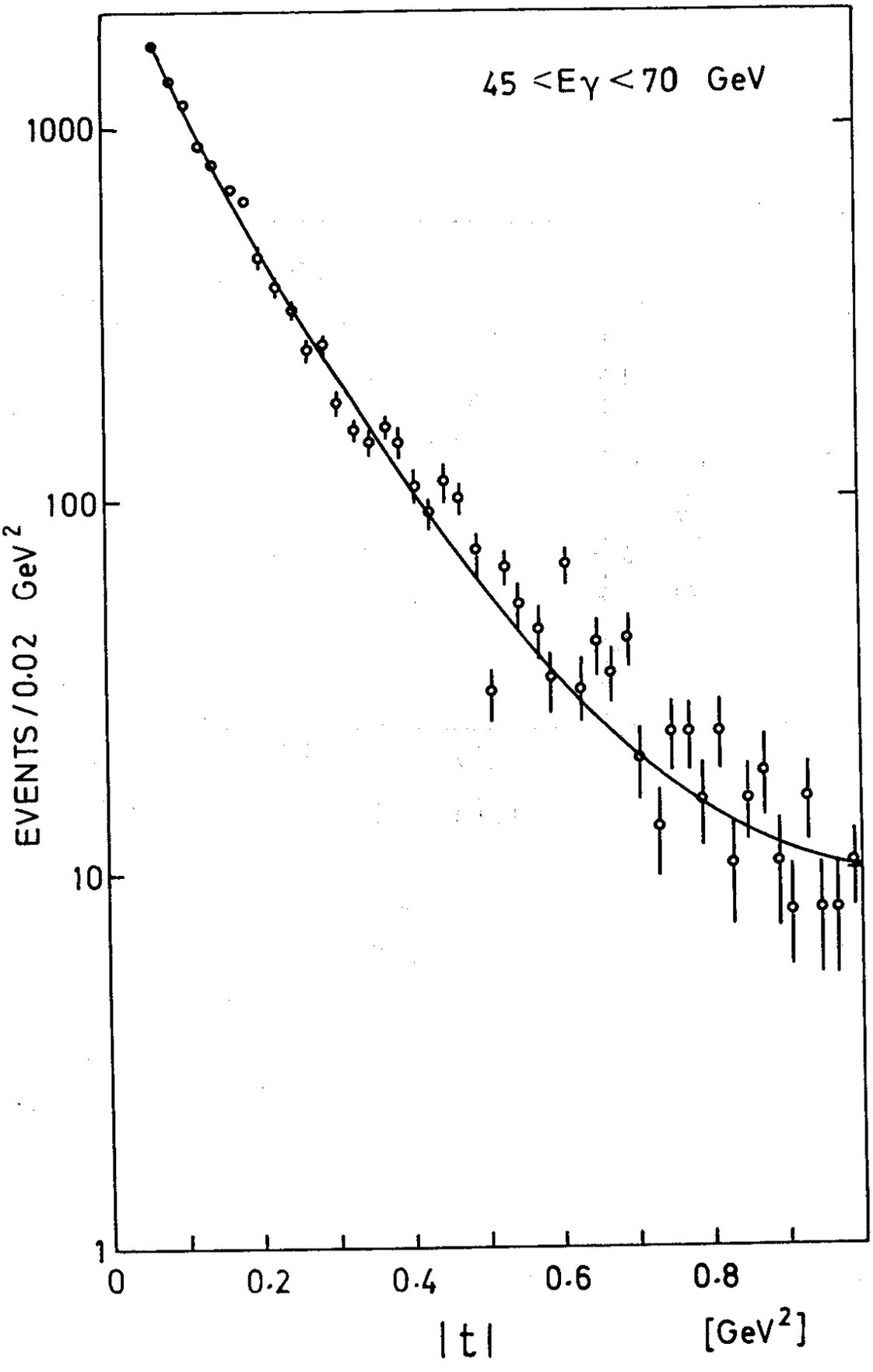

Fig. 5c

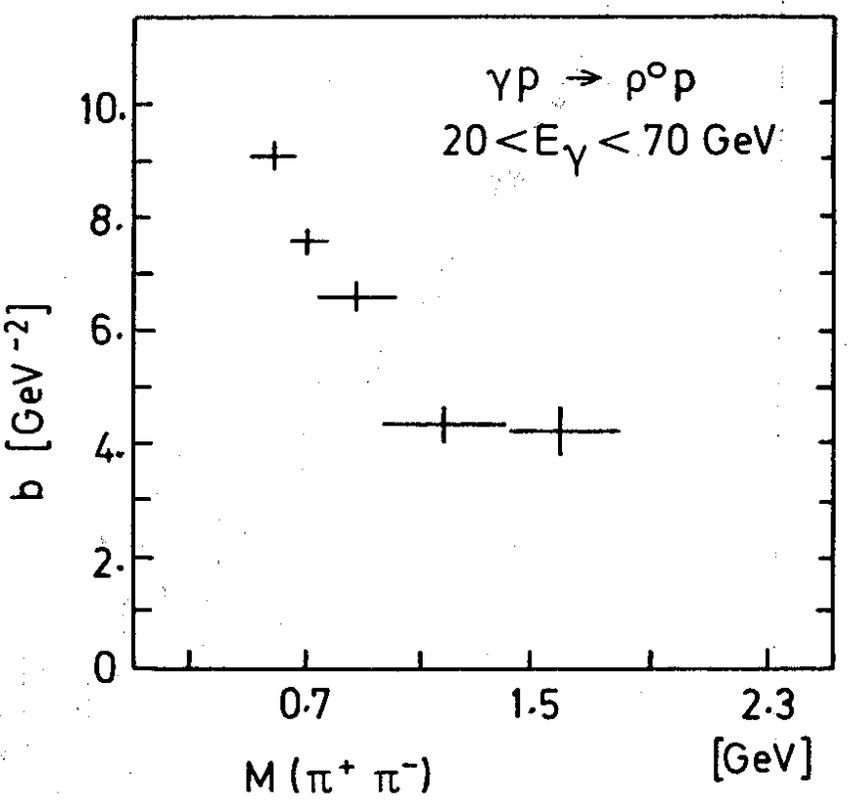

Fig. 6

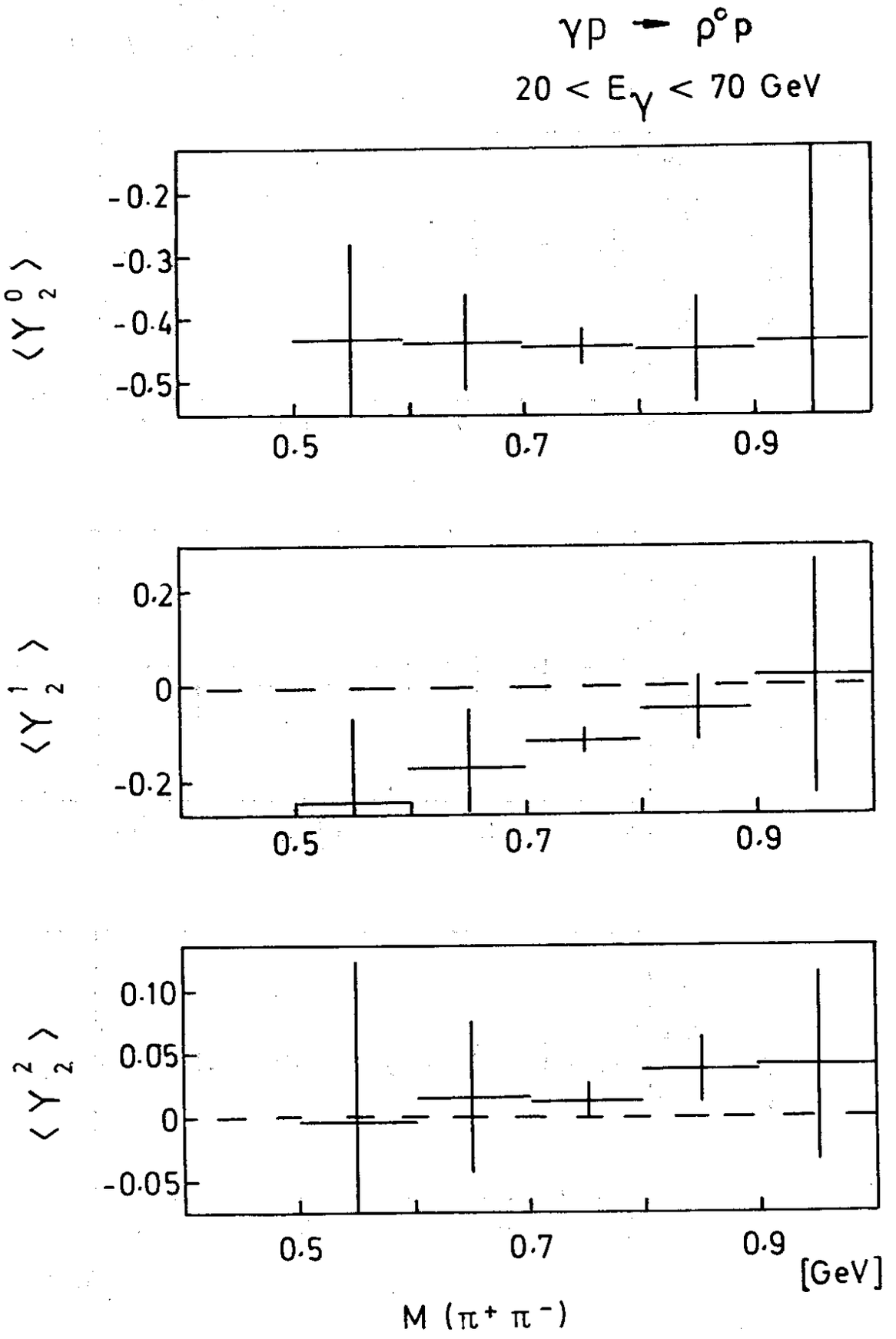
γp → ρ°p
20 < Eγ < 70 GeV
⟨Y 2 0⟩
-0.2
-0.3
-0.4
-0.5
0.5
0.7
0.9
⟨Y 2 1⟩
0.2
0
-0.2
0.5
0.7
0.9
⟨Y 2 2⟩
0.10
0.05
0
-0.05
0.5
0.7
0.9
[GeV]
M (π+ π-)

Fig. 7

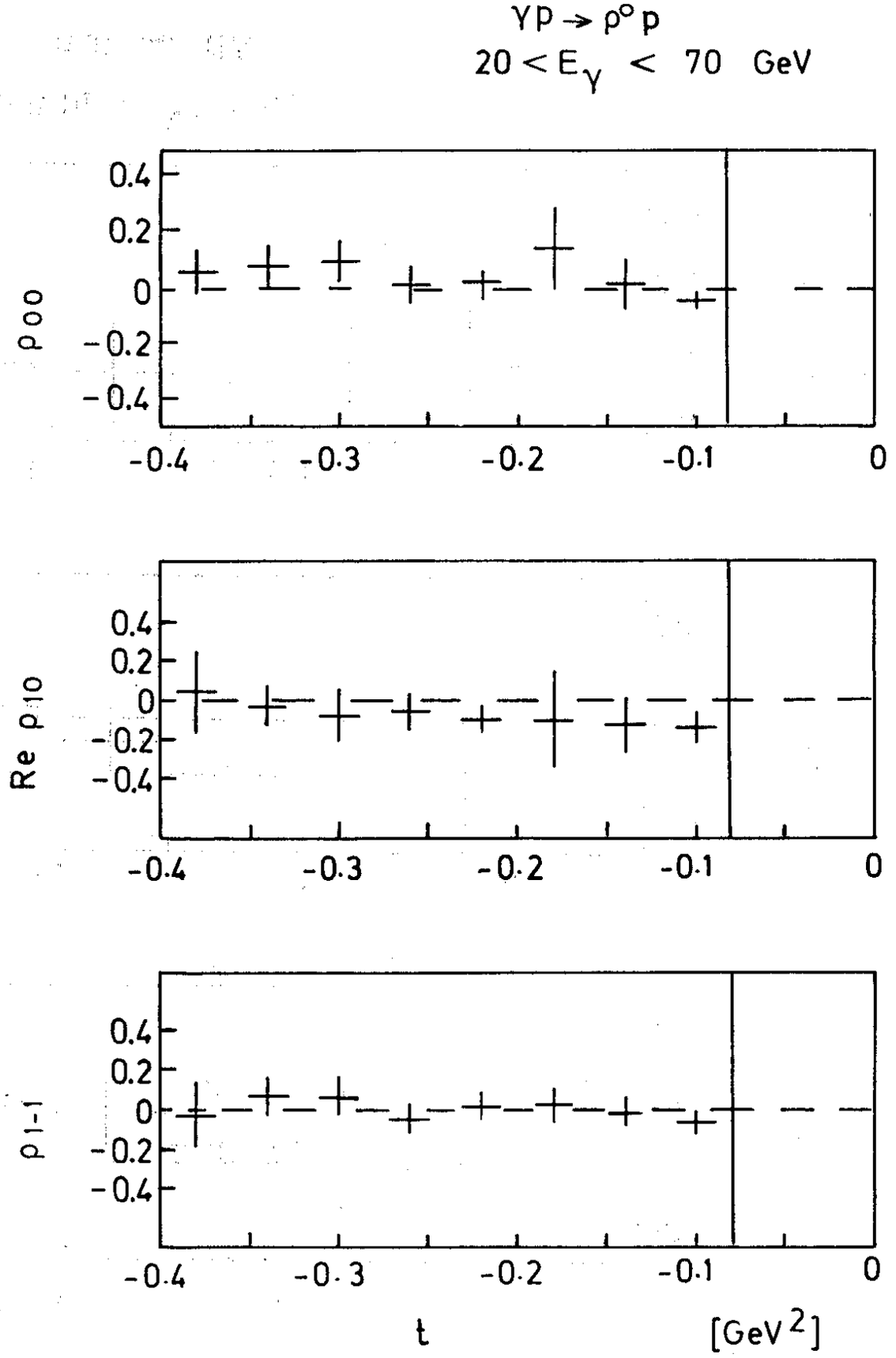

Fig. 8

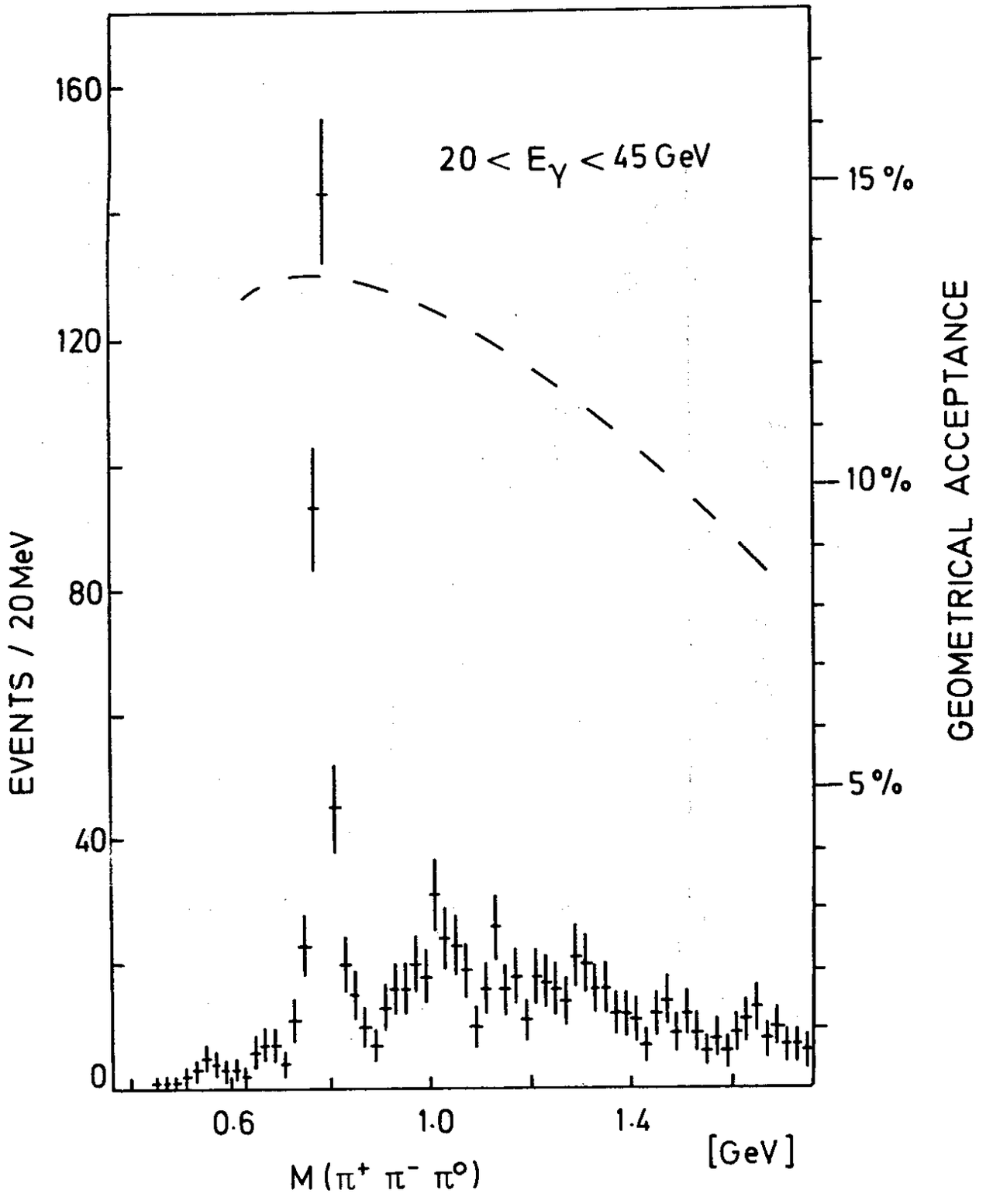
160
120
80
40
0
EVENTS / 20 MeV
20 < Eγ < 45 GeV
15 %
10 %
5 %
GEOMETRICAL ACCEPTANCE
0.6
1.0
1.4
[GeV]
M (π+ π- π°)

Fig. 9

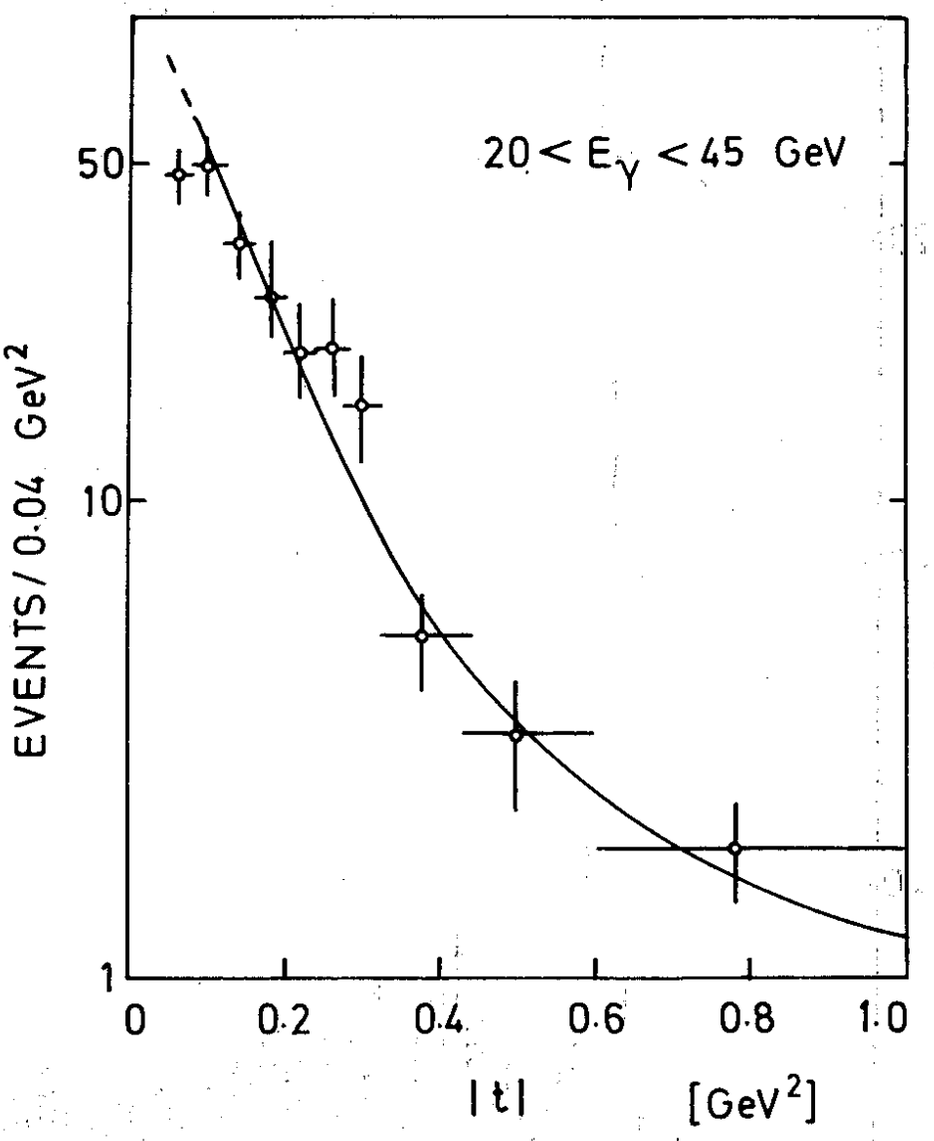

Fig. 10

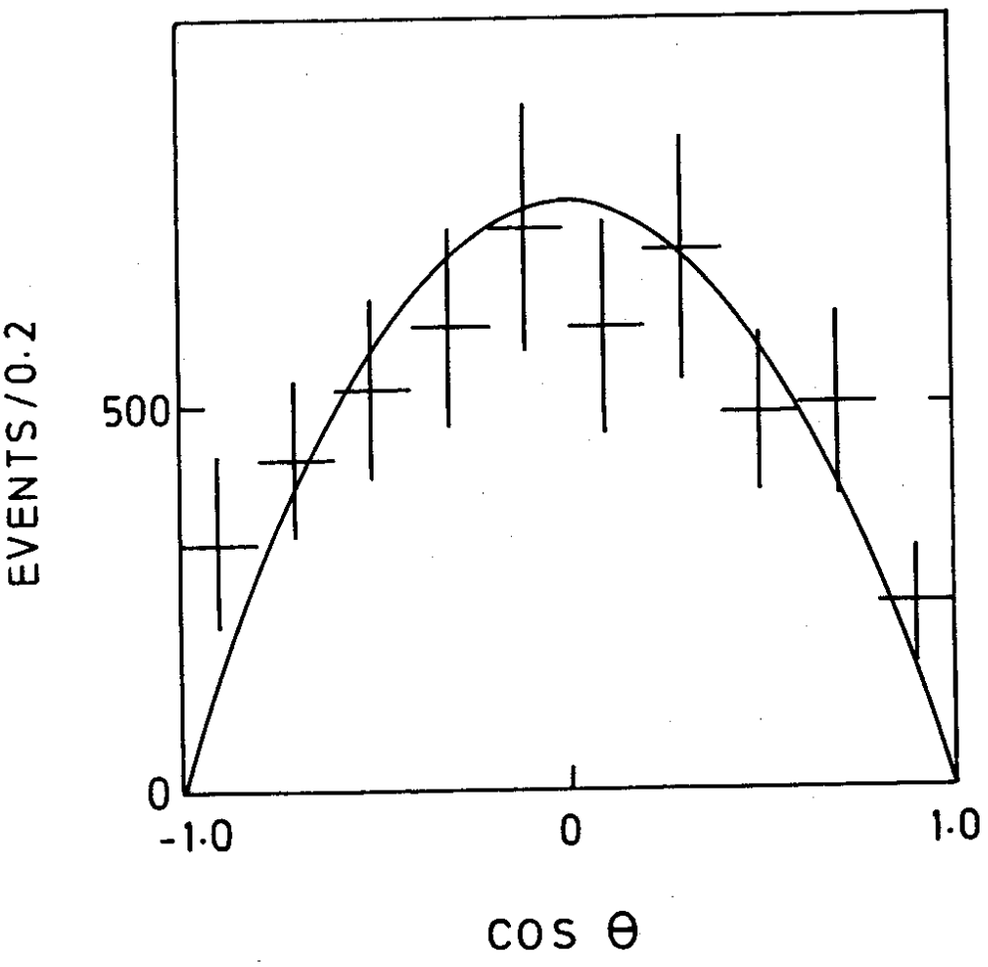

Fig. 11a

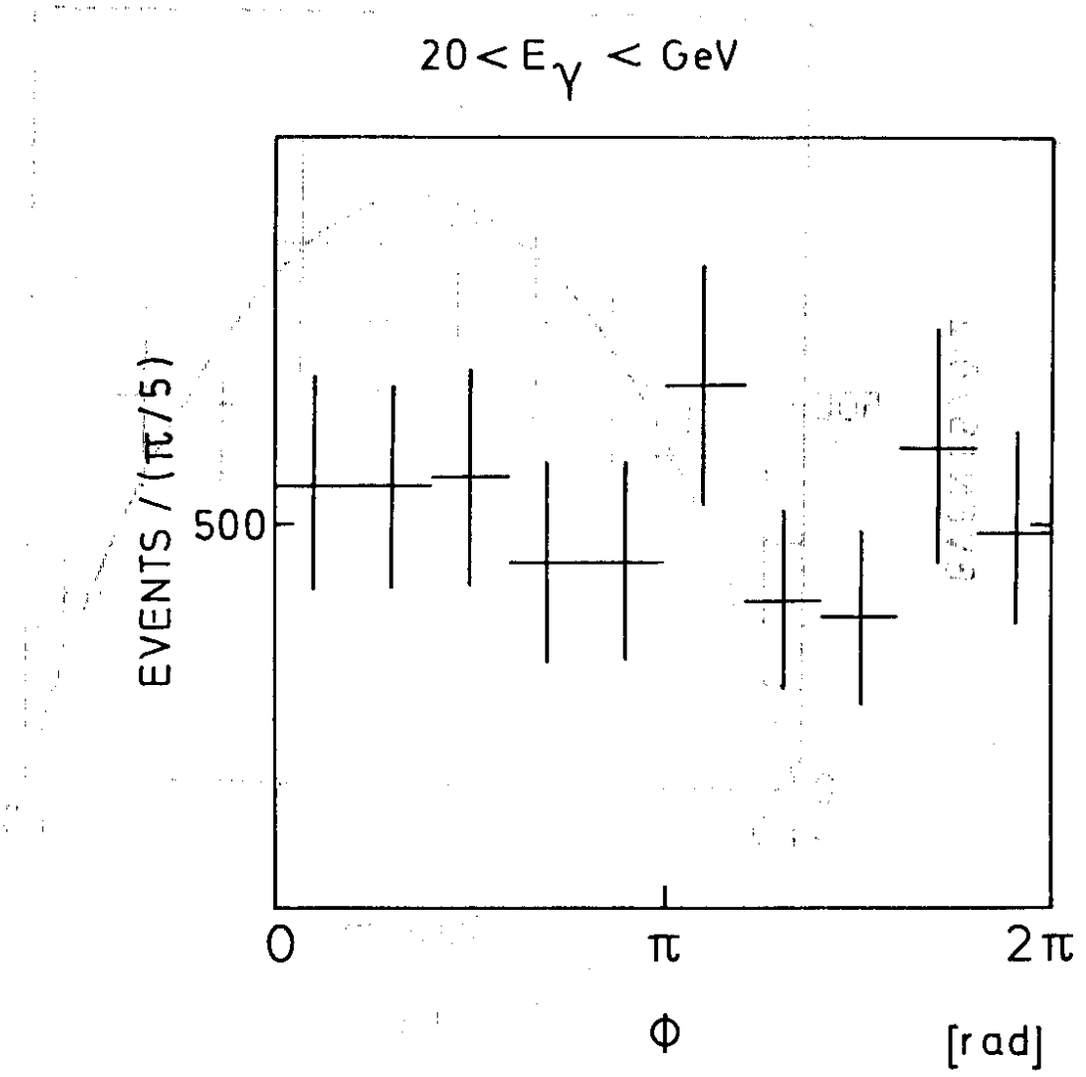

Fig. 11b

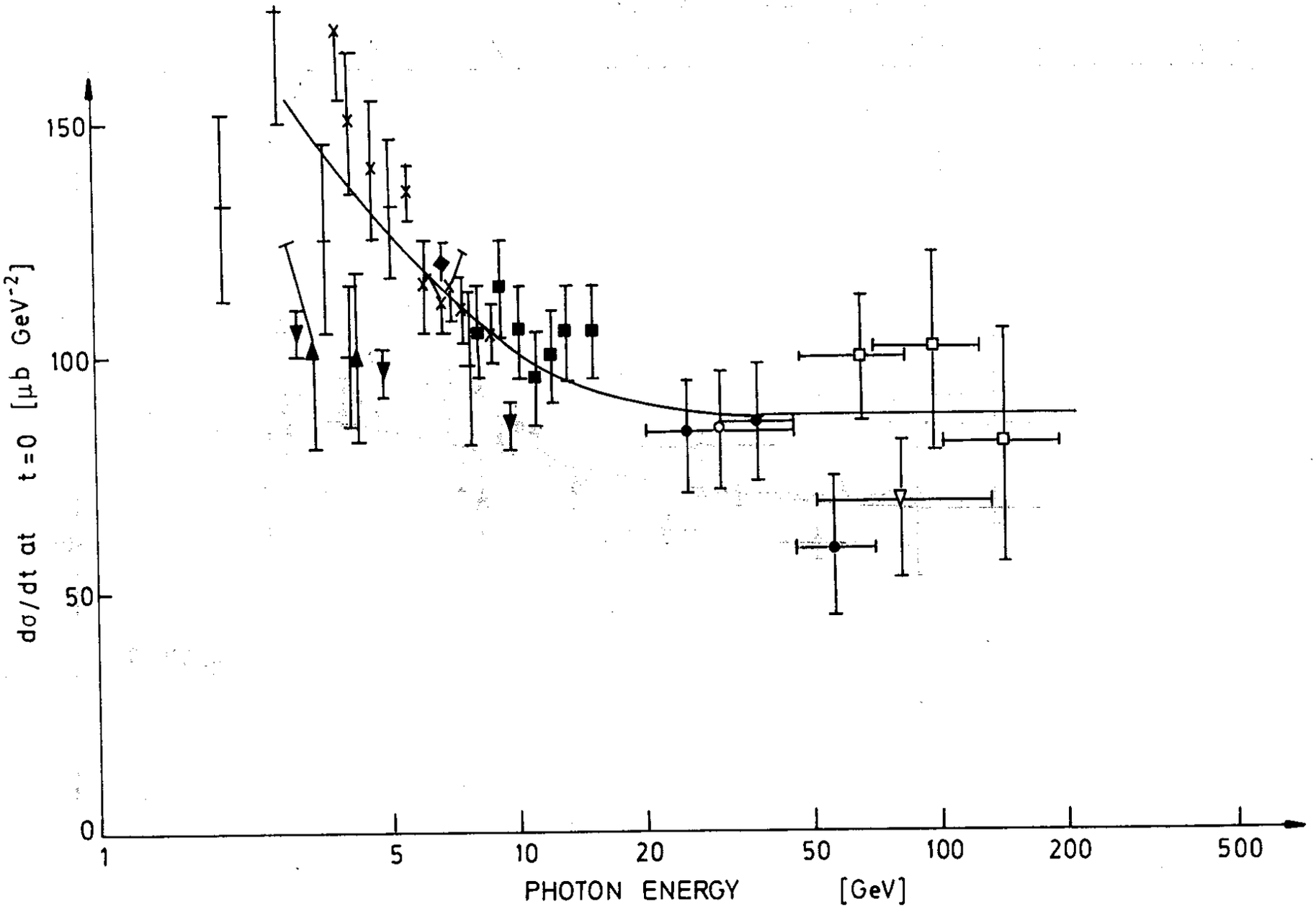
150
100
50
0
dσ/dt at t=0 [μb GeV⁻²]
1
5
10
20
50
100
200
500
PHOTON ENERGY [GeV]

Fig. 12a

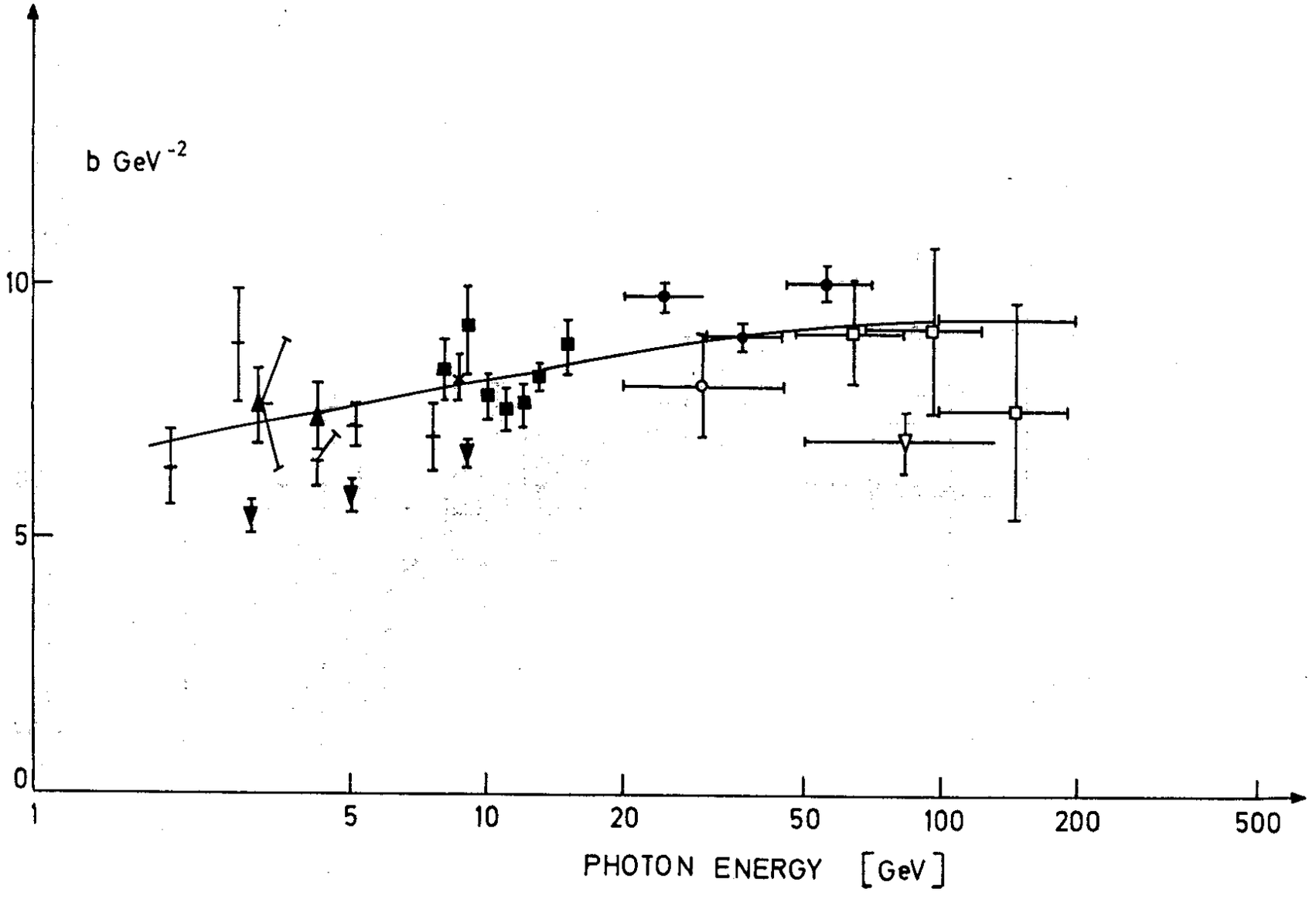

Fig. 12b